Proceedings of the 6th International Conference on Gas Hydrates (ICGH 2008),
Vancouver, British Columbia, CANADA, July 6-10, 2008.

NATURAL GAS HYDRATES UP CLOSE: A COMPARISON OF GRAIN CHARACTERISTICS OF SAMPLES FROM MARINE AND PERMAFROST ENVIRONMENTS AS REVEALED BY CRYOGENIC SEM

Laura A. Stern* and Stephen H. Kirby
U. S. Geological Survey
345 Middlefield Rd., MS/ 977
Menlo Park, CA 94025
USA

ABSTRACT

Using cryogenic SEM, we investigated the physical states of gas-hydrate-bearing samples recovered by drill core from several localities including the SE India margin (NGHP Expedition 01), Cascadia margin (IODP Leg 311), Gulf of Mexico (*RV Marion Dufresne* 2002), and Mackenzie River Delta (Mallik site, well 5L-38). Core material with a significant fraction of preserved hydrate has only been obtained for cryogenic SEM investigation from relatively few sites worldwide to date, yet certain consistent textural characteristics, as well as some clear differences between sites have been observed. Gas hydrate in cores recovered from Cascadia, Gulf of Mexico, and Mallik often occurs as a dense substrate with typical grain size of 30 to as large as 200 μm. The hydrate often contains a significant fraction of isolated macropores that are typically 5–100 μm in diameter and occupy 10-30 vol. % of the domain. In fine-grained sediment sections of marine samples, gas hydrate commonly forms small pods or lenses with clay platelets oriented sub-parallel around them, or as thin veins 50 to several hundred microns in thickness. In some sections, hydrate grains are delineated by a NaCl-bearing selvage that forms thin rinds along hydrate grain exteriors, presumably produced by salt exclusion during original hydrate formation. Preliminary assessment of India NGHP-01 samples shows some regions consistent with the observations described above, as well as other regions dominated by highly faceted crystals that line the walls or interior of cavities where the hydrate grows unimpeded. Here, we focus on gas hydrate grain morphology and microstructures, pore characteristics and distribution, and the nature of the hydrate/sediment grain contacts of the recovered samples, comparing them to each other and to laboratory-produced gas hydrates grown under known conditions.

Keywords: gas hydrate, scanning electron microscopy, grain characteristics

INTRODUCTION

Evaluation of gas hydrate grain and pore structures, and the nature of the hydrate grain contacts with sediments, remains an ongoing challenge in the study of natural gas hydrates. The amount, spatial distribution, fabric, and morphology of gas hydrates in nature not only influences the behavior of sediments or formations in which they occur, but also affects physical properties measured on recovered samples. Understanding the textural characteristics of samples is not trivial; the textures can be useful guides to *in situ* growth conditions, yet are easily altered by the effects of changes in environmental conditions, including those incurred during recovery and handling.

Cryogenic scanning electron microscopy (CSEM) offers an excellent means for obtaining such information, despite the technical challenges of maintaining samples at sufficiently low temperatures, avoiding water condensation during cold transfer, and minimizing electron beam damage of the imaging area. Distinguishing

*Corresponding author: Tel. 650.329.4811. lstern@usgs.gov

handling-induced surface artifacts from the intrinsic sample surface morphology can be difficult, or distinguishing hydrate from ice and determining the origin of the ice.

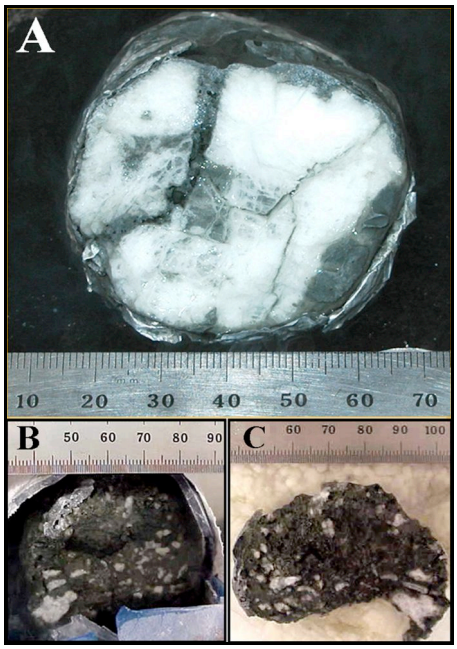

Figure 1. Macroscopic appearance of Cascadia margin samples 1328B (**image A**) collected from a cold vent site near the seafloor surface, and sample 1328E (**B**, **C**). XRD (Fig. 2) shows that the nodule is predominantly sI methane hydrate.

Imaging gas hydrates recovered from nature poses additional challenges as samples are at least partially decomposed or altered during drilling, transit to the surface, handling, and the preservation process. Even those samples retrieved by pressure corer undergo partial alteration when transferred to a different vessel at the surface or when frozen or re-pressurized under a different gas composition than that of *in situ* conditions. As such, they contain to varying degrees hydrate that may be partially changed from its original textural and composition state, or hydrate decomposition products, including ice, trapped gas, or frozen pore water. On a positive note, some of these issues are becoming less problematic as we continue to receive increasingly well preserved samples from new localities and build an increasingly larger archive of images. Comparing the observed features to those of lab-made hydrates of known composition and pressure-temperature history also aids in our interpretation of natural hydrates.

Use of CSEM for imaging gas hydrates has only been reported in the literature over the last decade, such as by Kuhs, Staykova, Klapproth, Genov, Techmer**,** and coworkers [1-7]. Our own group has also reported on SEM imaging of gas hydrates, including methane hydrate (± sediments) at various extents of reaction [8], dissociation and dissolution textures [8-10], compaction and deformation textures [11,12], propane, ethane, methane-ethane, and CO_2 hydrates [8-10,13], and natural gas hydrates from the Gulf of Mexico [14] and from the sub-arctic Mallik site [15]. We have also imaged hydrate-bearing samples with known fractions of ice, as well as samples used in partial decomposition tests [8-10] to address the question of distinguishing hydrate from ice.

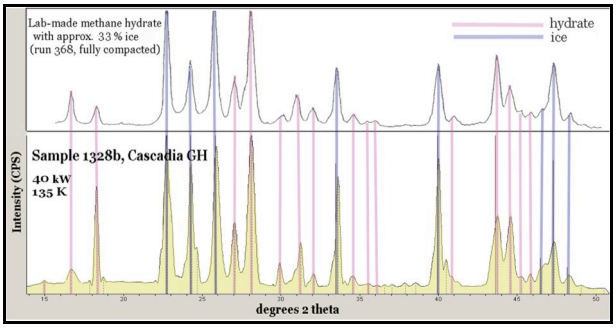

Figure 2. Comparison of x-ray diffraction patterns of lab-made methane hydrate + ice (67:33 vol. % each) and Cascadia sample 1328B. The scans show nearly the same proportion of phases in both samples.

Here, we build on our previous experience with the CSEM imaging technique to investigate the physical states of marine gas-hydrate-bearing cores retrieved from the Cascadia margin (IODP Expedition 311) and India (NGHP-01; K-G Basin), and compare them to hydrate produced in our lab and to samples retrieved by drill core from other natural environments including the Gulf of Mexico (Mississippi Canyon) and NW Canada (McKenzie River Delta; Mallik Well 5L-38). Key questions are: 1) What does natural gas hydrate from different localities look like? Specifically, what ranges of hydrate grain morphologies, micro-structures, and pore characteristics are observed, and how do they compare from site to site? 2) How does the gas hydrate interact with the sediment fraction, and how is it distributed? 3) How do lab samples aid in our interpretation of natural samples? 4) What features are artifacts of retrieval? In most cases, these questions are best answered by the images presented below of natural hydrates that illustrate some of the startling similarities and differences among samples from different localities.

EXPERIMENTAL METHODS

Transit. Samples we received from Cascadia and India were recovered by standard IODP coring systems and arrived in liquid nitrogen (LN) "dry" vapor shippers. Each sample or plastic-lined core was individually bagged or wrapped in Al foil. A small amount of free LN was present in the base of the shippers upon arrival, indicating that samples remained thermally stable during transit. Mallik and Gulf of Mexico samples [14, 15] were recovered by conventional coring as well.

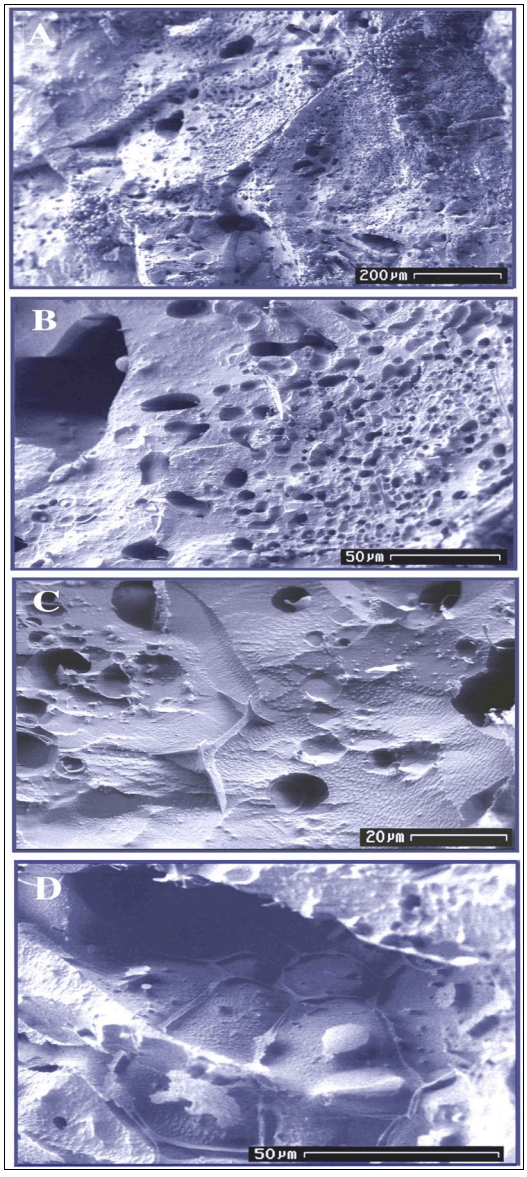

Figure 3. Substrate, grain, and pore structures of Cascadia 1328B from low (**A**) to high (**C**) magnification showing the general appearance of the hydrate as well as the size, abundance, and distribution of the pores. Grains in the dense hydrate substrate between the pores are typically 20-80 μm and are sometimes rimmed by NaCl (**C**, **D**), as shown also in Figs. 6- 9.

SEM sample imaging procedures. Small sections of samples (~0.5 cm x 0.5 cm x 0.75 cm) were cleaved under LN from the bulk samples, transferred to a sample stage within an evacuated and pre-chilled (<100 K) cryo-preparation and coating station (Gatan Alto Model 2100), which in turn attached to a LEO 982 field emission SEM. In the preparation chamber, samples were again cleaved by cold blade to produce fresh fracture surfaces that were not contaminated by surface-water condensation. While still under vacuum,

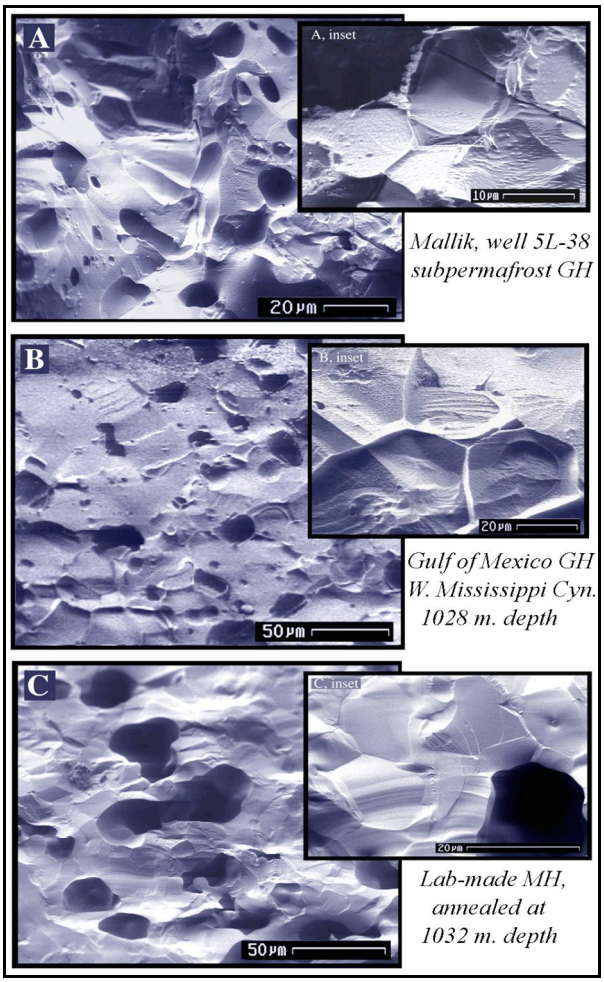

Figure 4. Substrate, grain, and pore structures in gas hydrate from other environments for comparison with Cascadia hydrate shown in Fig. 3. Panel **A:** sub-arctic gas hydrate from the Mallik site, NW Canada; **B:** marine hydrate retrieved from the Gulf of Mexico; **C**: lab-made methane hydrate that was then annealed at the ocean floor [8,10]. All samples exhibit pervasive and isolated macropores within an otherwise dense hydrate substrate. Insets show magnified views where grain boundaries are delineated. Grains are commonly several tens of microns in diameter, even in the lab hydrate (**C**) that was finely crystalline (see Fig. 5C) prior to seafloor annealing.

samples were inserted directly through the back of the preparation chamber and on to an auxiliary cryo-imaging stage in the SEM column. Temperature was monitored by a thermocouple embedded in the stage just below the sample, and imaging was conducted at temperature below 102 K and vacuum below 10^{-6} kPa (10^{-5}mbar). Low accelerating voltage (2kV) was used to minimize sample alteration or beam damage to the sample surface, increasing to 10 kV only for EDS procedures (described below.) Further details of imaging procedures are given in [8] and [10]. In some cases, samples were first imaged by x-ray computed tomography (CT) at Lawrence Berkeley Laboratory before being sectioned for SEM work in order to non-invasively determine the distribution and location of the gas hydrate within large cores. One sample was imaged by SEM both before and after CT imaging to ensure that no changes occurred during the CT procedures.

In the SEM column, gas hydrate was distinguished from ice using the instrument's energy dispersive x-ray spectroscopy (EDS) capabilities, which identified small but distinct carbon peaks when focused on flat, dense, non-dissociated hydrate surfaces. EDS was also used to identify Na and Cl peaks in salt observed in some samples. Several nodules of hydrate were also analyzed at low temperature by powder x-ray diffraction and compared to known samples and standards.

RESULTS AND DISCUSSION

Comparing gas hydrate in pure or massive form. Despite the diverse global settings from which the gas hydrate samples and cores were retrieved, a surprising number of similarities were observed, particularly when comparing hydrate that occurs as lenses, pods, nodules, or in similar massive and relatively pure form such as those shown in Figure 1. In such cases the grain and pore characteristics exhibit a markedly self-consistent appearance, with the hydrate phase forming a dense (i.e. not nanoporous) substrate with grains typically 30-80 μm in diameter (Figs. 3-7) and sometimes ranging up to 200 μm. Recent work by Klapp et al. [16] suggests that natural gas hydrate grain sizes may in fact largely cluster in the 300-600 μm range, with larger sizes correlating with depth, but we do not have a sufficient inventory of samples, and particularly those from depth, to comment on this finding.

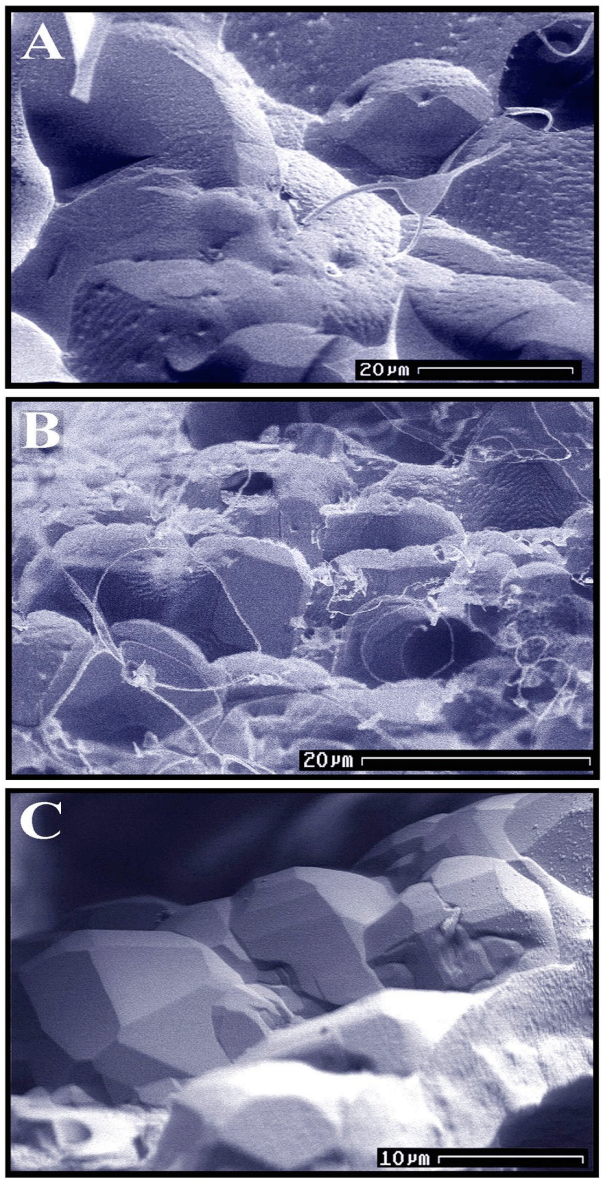

Figure 5. Well developed gas hydrate crystals often line the pores of the exposed surfaces of nodular gas hydrate. **A** shows crystalline hydrate from Cascadia sample 1328B, and **B** shows crystalline hydrate lining an exposed surface of India NGHP-01 sample HYD55. Lab-made methane hydrate grown by methods discussed in [8] is shown in **C**, displaying similar grain size, habit, and dense substrate.

All gas hydrate samples and cores reported here also contained numerous and typically isolated macropores that account for roughly 10 to 30 volume % of the domain (Figs. 3, 4, and 7.) In some cases, such as in samples retrieved from the Gulf of Mexico, obvious dissolution or partial dissociation features were observed that precluded determination of whether the pores were original features. In samples recovered from Cascadia and

India however, hydrate crystal faces were often observed along the pore interiors or exposed surfaces (Figs. 5–7) suggesting that the macropores and cavities are for the most part original features and not a product of dissolution or dissociation. The crystal faces are typically quite fine and range several tens of microns at most (Fig. 5A, B), and in fact resemble the crystalline gas hydrate formed in the laboratory at high temperature under excess gas conditions (Fig. 5C). Some ice does occur in the recovered nodules from all localities, however, as is apparent from both SEM examination and XRD analysis (Fig. 2).

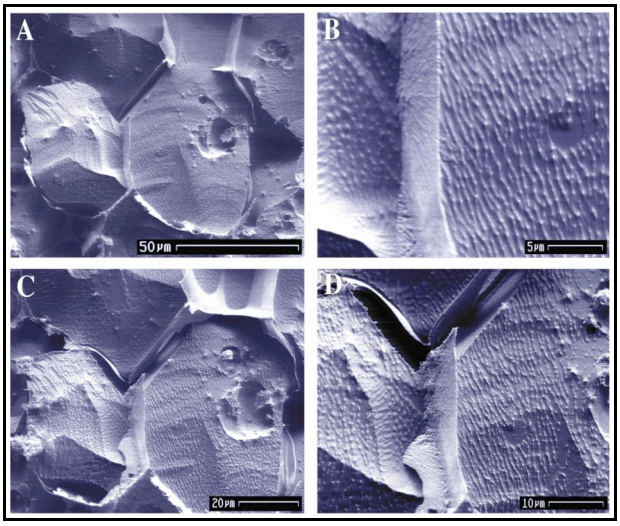

Figure 6. Individual gas hydrate grains in Cascadia sample 1328B are often rimmed by a boundary material that becomes increasing exposed as the gas hydrate sublimates. Time lapse from image **A** and detail **B**, to image **C** and detail **D**, is 25 minutes.

In many of the samples recovered from marine environments (Gulf of Mexico, Cascadia and India), gas hydrate grains are often delineated or bounded by a resistant material that forms thin rinds at hydrate grain exteriors and that becomes increasingly revealed as the interior hydrate sublimates (Figs. 3C, 3D, 6, 7, 8). The boundary material is often embedded well within the samples, and is not merely a surface feature. The material was identified in India samples by EDS as containing Na and Cl, with no other peaks appearing in the spectra except for carbon and oxygen from the background hydrate, and is thus identified as salt, or possibly NaCl dihydrate (Fig. 8).

Comparing gas hydrate + sediment sections. Despite the many similarities in the massive gas hydrate or nodules described above from the various localities, many striking differences emerge as well, particularly when comparing the mixed hydrate + sediment sections. In Cascadia samples, for instance, sediment sections commonly include small pods, lenses, or thin veins of hydrate that are surrounded by silt and clay platelets (Figs. 9 and 10). These sections also often exhibit rims of NaCl intermixed with fine sediment that forms a honeycomb-like matrix around the hydrate (Fig. 9). We presume that these boundary rims form by NaCl exclusion during original hydrate grain growth, suggesting that they are indeed original formation features. The hydrate within these pods is found to be dense (Fig. 9C, 10A) and exhibits carbon in its EDS spectra, and does not show signs of prior decomposition or other evidence to suggest alteration from its original texture. In other sections, lenses of gas hydrate are surrounded primarily by clay platelets that enclose the hydrate into small pods of 10 to 200 μm (Fig. 10A), around which the platelets are oriented in sub-parallel fashion (Fig. 10B, 10C)

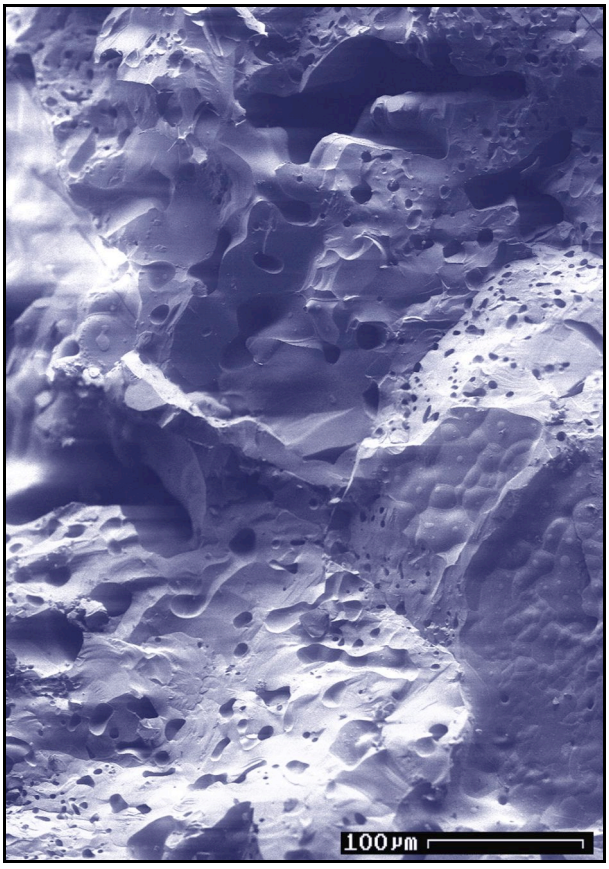

Figure 7. A predominantly methane hydrate nodule from India (NGHP HYD 82) showing the dense hydrate substrate with many isolated macropores similar to samples from other localities as well as annealed lab samples (Figs. 3, 4). Fig. 8 shows a detail of the lower-right section of this image.

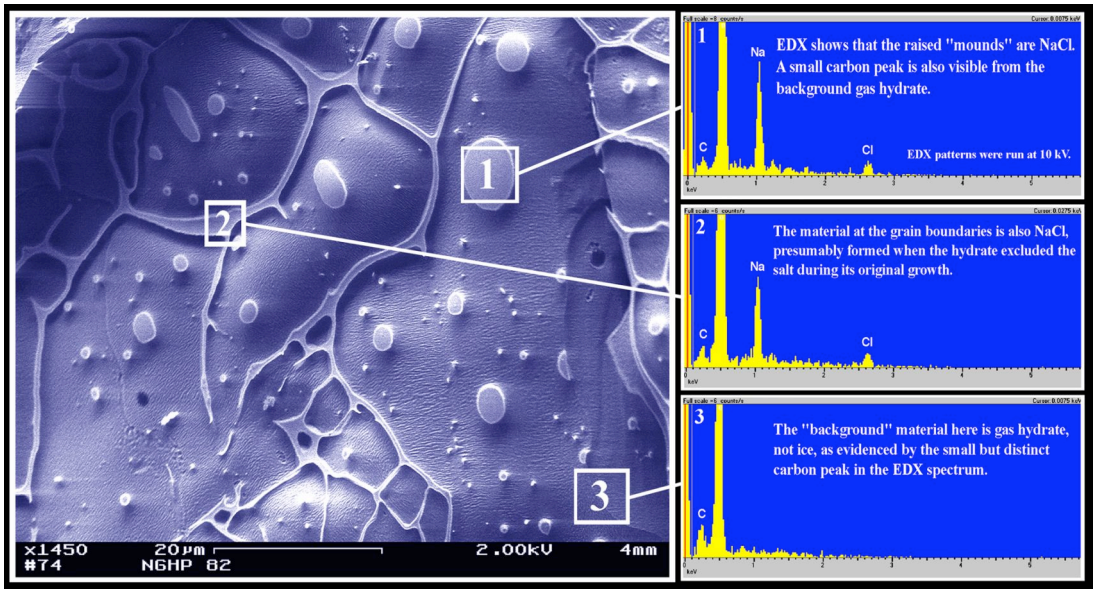

Figure 8. A boundary material that rims many hydrate grains and best exposed after hydrate sublimation is commonly observed in nodules from India NGHP-01. Shown here is NGHP sample HYD 82. EDS indicates these rims are salt, or possibly $NaCl{\cdot}2H_2O$ (NaCl dihydrate) based on the Na and Cl peaks in the spectra (panels 1 and 2 at right), and identifies the background phase as gas hydrate, not ice (panel 3.) Similar grain boundary material was also observed in samples from Cascadia and Gulf of Mexico, often mixed with sediments (Fig. 9).

We cannot tell at this point if the lenses and pods of hydrate are single crystal or polycrystalline, as it is difficult to distinguish grain boundaries within them. We found no evidence for hydrate grains much larger than 200 µm, but this may be due to the sampling procedures and the relatively few samples that have been recovered for SEM examination to date. In any case, the rapid sublimation of the hydrate phase under the SEM column reveals the 3-dimensional framework of these sections (Fig. 10B, 10C.) Sublimation was also used to observe other hydrate/sediment fabrics in various samples, such as brecciated sediment sections after thin veins of hydrate sublimated.

Gas hydrate + sand sections from samples collected from Mallik well 5L-38 have a distinctly different texture due to the large size of the sediment grains and the sometimes high percentage of hydrate matrix. These samples are described in [15] and a representative image is shown in Figure 11. Individual hydrate grains were difficult to distinguish and the hydrate was partially decomposed, but cores were still useful for information on phase distribution (Fig. 11).

Cores from India NGHP-01 provided some of the most interesting and well preserved hydrate to date. These samples exhibited a wide distribution of finely crystalline gas hydrate that lined cavity walls within the sediment sections of nearly all samples examined (Figs. 12-15). In all such cases, the gas hydrate was closely intergrown with the sediment and clays below, but growing unimpeded into sometimes astonishingly euhedral forms. Despite some unusual crystal habits, the hydrate was identified by its rapid sublimation compared to ice, it's fragility under the beam after only several seconds (Fig. 15C), the characteristic mottled or mesoporous surface it develops during deterioration under the beam (Figs. 14C, 15C), and the distinctive carbon peak in its EDS spectra. Loose, hexagonal platelets of ice were found in some samples, but the hydrate sometimes even exhibited pseudo-hexagonal forms that not only sublimated or altered rapidly under the beam, but that also exhibited a carbon peak (Fig. 13), hence distinguishing it from ice. Time lapse image sequences also distinguished hydrate from ice.

Analysis of cores from India and Cascadia also showed hydrate-bearing sections that contained minor to significant fractions of skeletal material. In some samples the hydrate developed in "massive" form between the fragments, such that hydrate grain boundaries were not resolvable. The hydrate then sublimated to reveal remarkably well preserved skeletal material below (Figs. 16, 17A). These sections often contained clusters of framboidal pyrite as well (Fig. 17B).

Recovery features. One aspect where ocean floor annealing and recovery tests of lab-made hydrate have proved fruitful is in identification of textures produced during the recovery process. We have seen in all recovered samples to date that gas hydrate grain boundaries near or at the sample surface are often replaced by a skeletal polyhedral foam material (Fig. 18.) This material stands out above the hydrate, and is believed to be frothy ice produced by hydrate decomposition along the boundary that is then quenched in liquid nitrogen. These structures are too fragile for close inspection by SEM, but based on their development in lab-made samples sent to and retrieved from the ocean floor, we can identify them with reasonable confidence as a dissociation byproduct (ice), as they also form in known samples made from fresh water with no added sediments or salts (Fig. 18D). Nearly identical foam textures are formed by quenching of rapidly degassing volcanic melts [17].

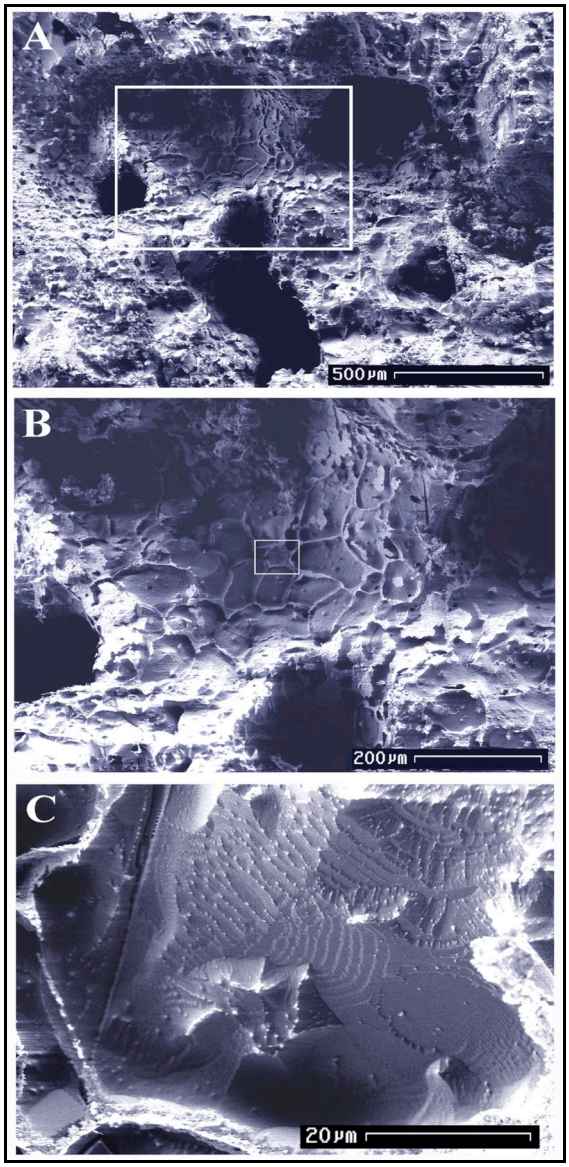

Figure 9: A gas hydrate/sediment section from Cascadia sample 1328E, showing a honeycomb-like framework of gas hydrate rimmed by silt and clay platelets. Outlined boxes in **A** and **B** are enlarged in **B** and **C** respectively. The initially dense, nonporous nature of the hydrate is shown in **C**. A similar framework is also seen in non-sediment portions of the sample, suggesting that salt crusts compose some of the boundary material here as well (Figs. 7, 8),

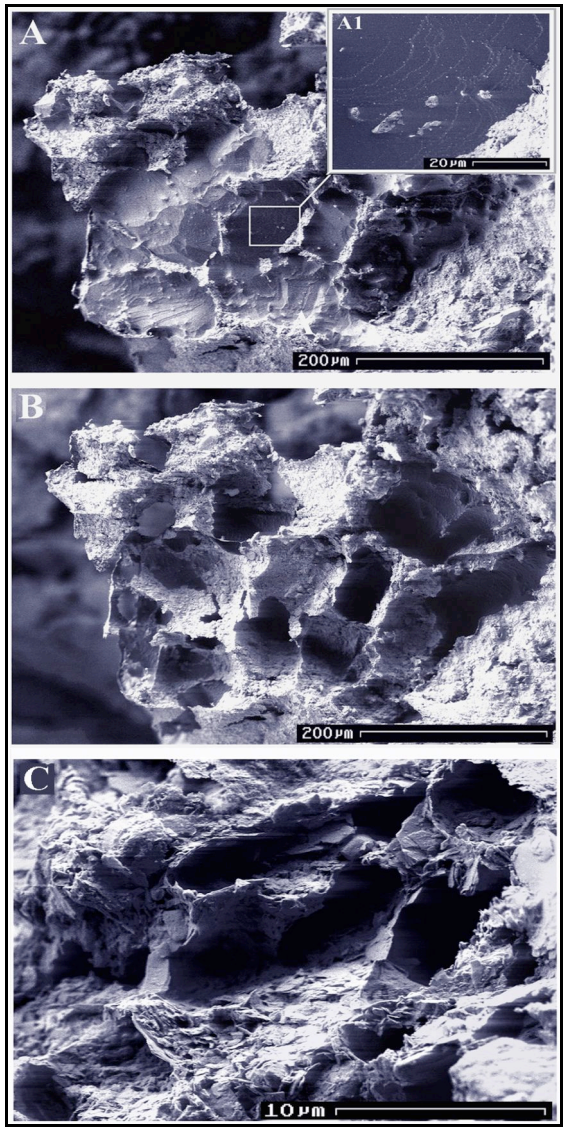

Figure 10. Sublimation effects on Cascadia sample 1328E. Image **A** shows a section immediately after entry to the SEM column. The dense hydrate substrate is shown in inset **AI**. **B** shows the same section 40 minutes later after the gas hydrate sublimated, revealing a 3-dimensional view of the lens-like regions originally occupied by hydrate. Clay platelets commonly orient sub-parallel around the lenses (**C**).

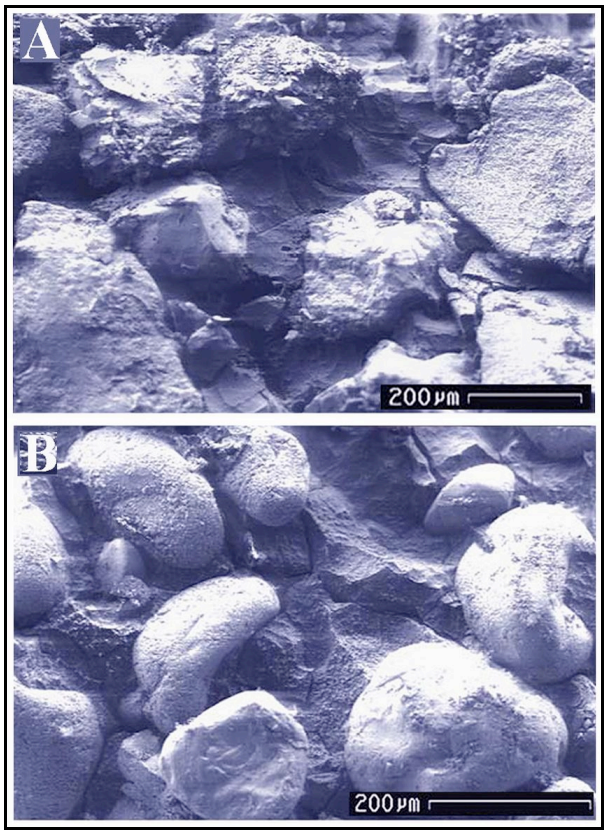

Figure 11 (***at left***.) Gas hydrate + sand mixtures. **A** is a representative image of a sub-permafrost gas hydrate + sand section from Mallik Well 5L-38 (sample 107358.) The gas hydrate (grey material between the sand grains) has partially decomposed to ice, rendering the sample poorly suited for physical properties testing but useful for information on phase distribution (see also [15]). For comparison, a lab-synthesized pure methane hydrate + quartz sample, made for material properties testing of known mixtures, is shown in **B**. Tests on lab samples show that methane hydrate is significantly stronger that water ice, and hydrate/sand mixtures are similarly stronger than ice/sand mixtures ([11], [12], [15]).

Figure 12 (*below*). Nearly all of the India NGHP-01 cores exhibit a network of cavities, pores, or vugs lined with crystalline gas hydrate attached to the sediment below and growing unimpeded into euhedral forms and exhibiting a wide variety of crystal habits. Initially considered to be an artifact of the recovery process, the prevalence of this type of hydrate growth found in these samples suggests otherwise. Shown here is HYD 29.

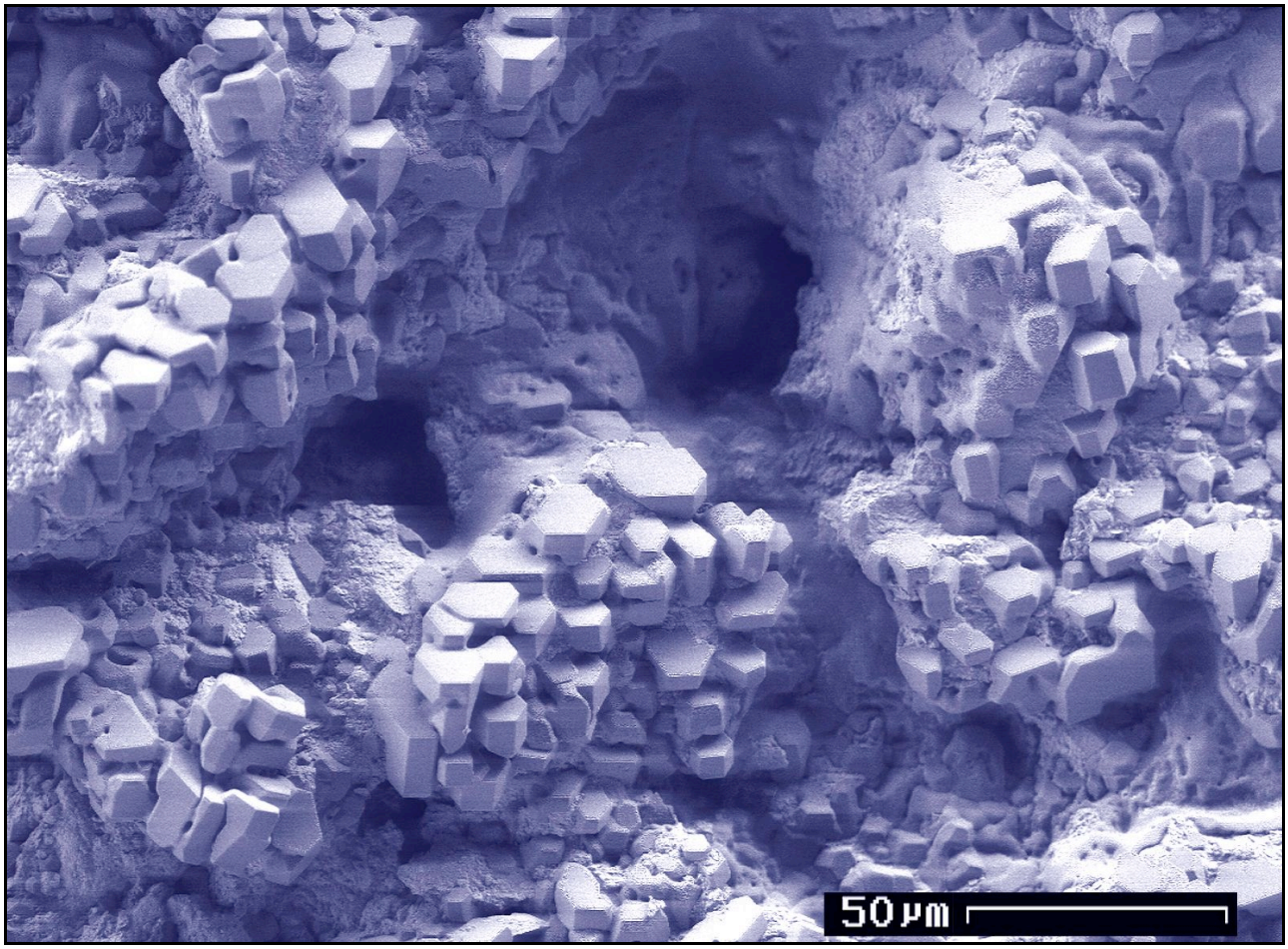

SUMMARY AND CONCLUSION

SEM serves as a powerful tool not only for investigating the progress of gas-hydrate-forming reactions and the consequent development of grain and pore structures, but also for enabling close examination of the morphology and grain contacts in samples from nature, and for making relevant comparisons to hydrates made and tested in the laboratory. We have previously shown, for example, how growth textures of gas hydrate made from ice evolve and anneal as reaction reaches completion at high pressure and temperature conditions, producing dense clusters of grains with prominent crystal face development ([8, 10], also Fig. 5c.) Significant changes in pore shapes and connectivity also accompany the growth process, and the relatively simple geometry of the initial ice reactant develops into a far more complex arrangement in the final hydrate product.

SEM also provides a excellent means for determining how closely synthetic samples emulate those from nature. Gas hydrate + sand aggregates can be synthesized to yield similar textures and phase distribution to those found in sand intervals in sub-permafrost settings, for instance, as shown in Figure 11. This is encouraging for physical properties specialists, as lab-made samples may contain known phases and phase distribution, compared with the complexity and unknown ice fraction in samples from nature.

We have also shown that even short-term exposure of lab synthesized hydrate to oceanic conditions within the nominal gas hydrate stability zone can induce extensive morphological changes in the

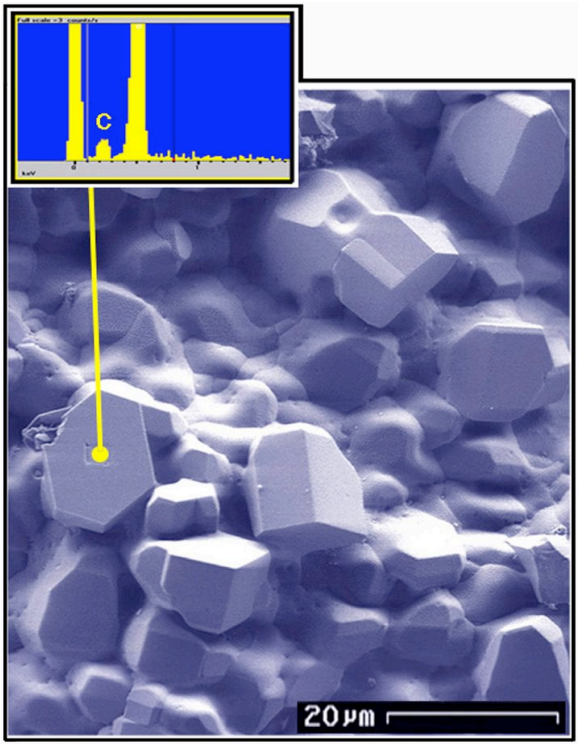

Figure 13. Gas hydrate crystals lining a cavity wall in India NGHP-01 core HYD 29. A variety of crystalline habits are exhibited, including some pseudo-hexagonal platelets that resemble ice. While secondary ice does occur in some samples, the crystals here exhibit a carbon peak in their EDS spectra and behave in the characteristic fragile manner of hydrate under the beam.

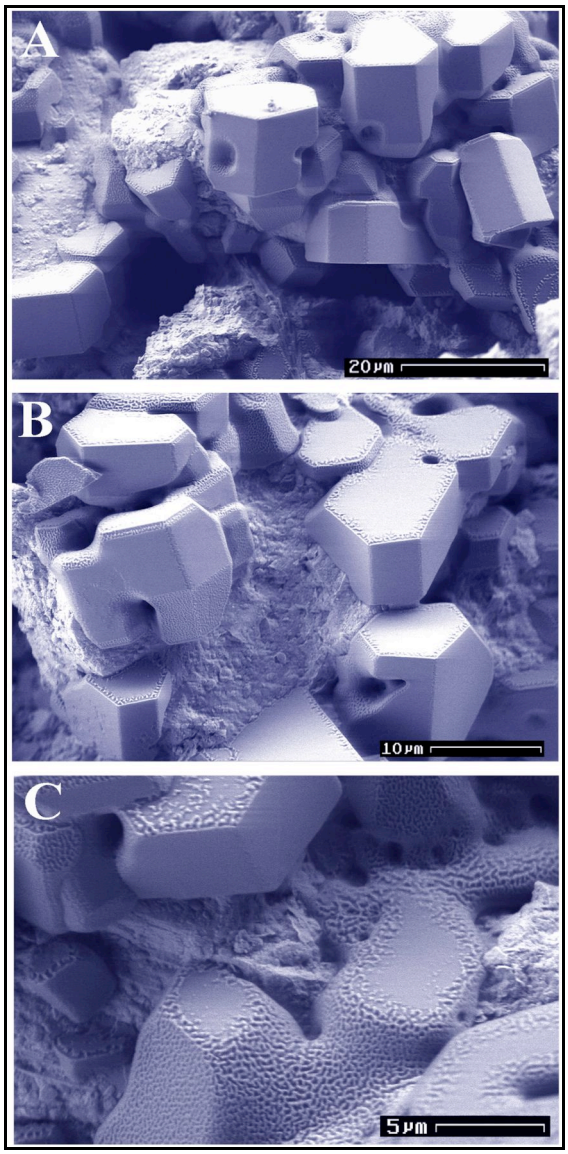

Figure 14. Other sections of India HYD 29 showing the variety of gas hydrate crystal habits and the manner in which they grow unimpeded into open cavities. **C** shows the characteristic deterioration of hydrate crystal surfaces under the SEM beam, developing a sponge-like surface texture.

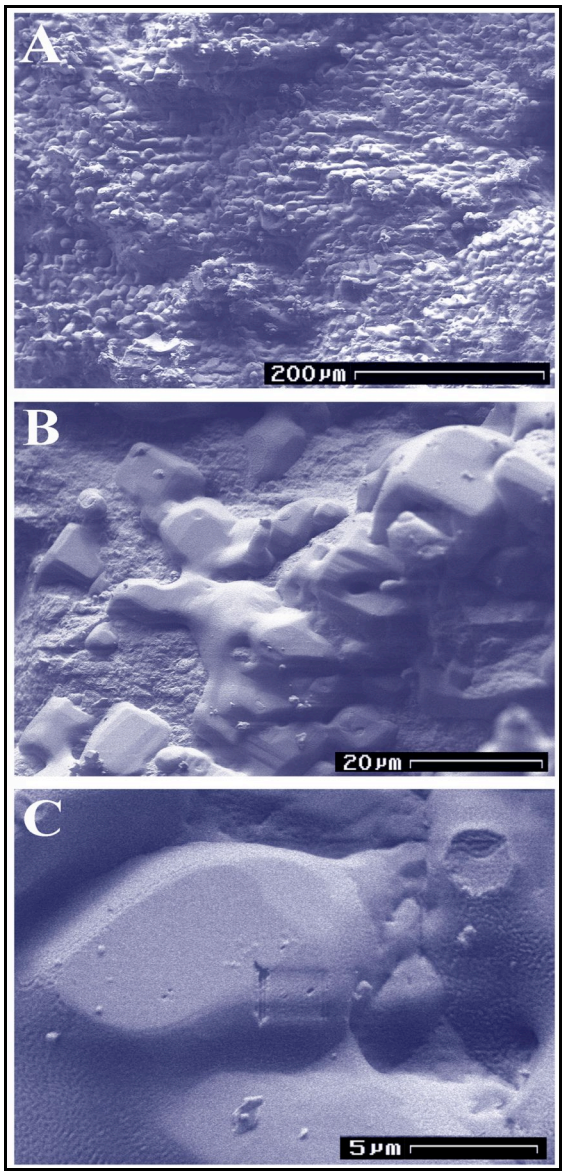

Figure 15. A section of India sample HYD 7 from low (**A**) to high (**B, C**) magnification, showing other views of crystalline gas hydrate growth. **C** shows the characteristic rapid burning under the beam and the uneven surface that develops with sublimation.

hydrate, such that it may in fact closely mimic textures observed in natural marine hydrate retrieved from comparable depths ([9], also Fig. 4B *vs.* 4C). Grain and pore characteristics converge to a fairly uniform appearance with a dense hydrate substrate comprised of grains typically 30-80 μm, riddled with mostly isolated macropores that account for ~ 10 to 30 vol. % of the domain (Figs. 3, 4, 6). These consistencies are encouraging as they lend increased confidence to the extrapolation of measurements made on lab-synthesized-and-annealed gas hydrate to gas hydrates in nature. Stoichiometry changes that accompany annealing can also bring the lab-made hydrates in closer alignment with those from nature [18].

One of the more unexpected findings was the prevalence of finely crystalline gas hydrate lining many pores and along exposed surfaces of large nodules of gas hydrate (Figs. 5, 6.) Even more remarkable was the widespread distribution of finely crystalline gas hydrate lining cavity walls within the sediment sections of samples (Figs. 12-16D). In this latter case, the hydrate appears closely intermixed with the sediment and clays below, yet grows unimpeded into sometimes astonishingly euhedral forms and displays a wide range of crystal habits. In some instances ice was also found in these sections, but the gas hydrate could be easily identified by its rapid sublimation compared to ice, its instability under the beam (Fig. 15C), the characteristic uneven or nanoporous surface it develops under vacuum (Fig. 14C, 15C), it's crystal habits and forms (Figs. 12-15), and the small-but-distinctive carbon peak present in its EDS spectra (Figs. 8, 13).

We have also now identified the boundary material that forms thin, resistant rinds at hydrate grain exteriors, and that becomes increasingly revealed as the interior hydrate sublimates (Figs. 3C, 3D, 7, and 8). These rinds occur in samples from multiple localities, and we show here that they are primarily made up of salt or $NaCl{\cdot}2H_2O$ (Fig. 8), or intermixed with sediments to form a honeycomb-like matrix around the hydrate (Fig. 9). We presume that these rims form by salt exclusion during original hydrate grain growth, and that they are indeed original features rather than a decomposition product. In other sections, only the sediment particles surround the hydrate, often enclosing the hydrate into small pods of 10 to 200 μm (Fig. 10A) around which clay platelets are loosely oriented (Fig. 10B, 10C.) It is difficult to tell at this point if the larger pods are single crystal or polycrystalline, but we can at least establish the 3-dimensional framework of these sections after the hydrate sublimates (Fig. 10B).

Analysis of gas hydrate samples from Cascadia and India also show that the sediment in which the gas hydrate forms often contains significant fractions of skeletal material or other bio-mass in addition to silt and clay fragments. In some samples, the hydrate occurs in "massive" form between the fragments, such that hydrate grain boundaries are not defined. It sublimates rapidly

however, revealing the skeletal material below (Figs. 16, 17). Finely crystalline hydrate is also found in these samples (Fig. 16D).

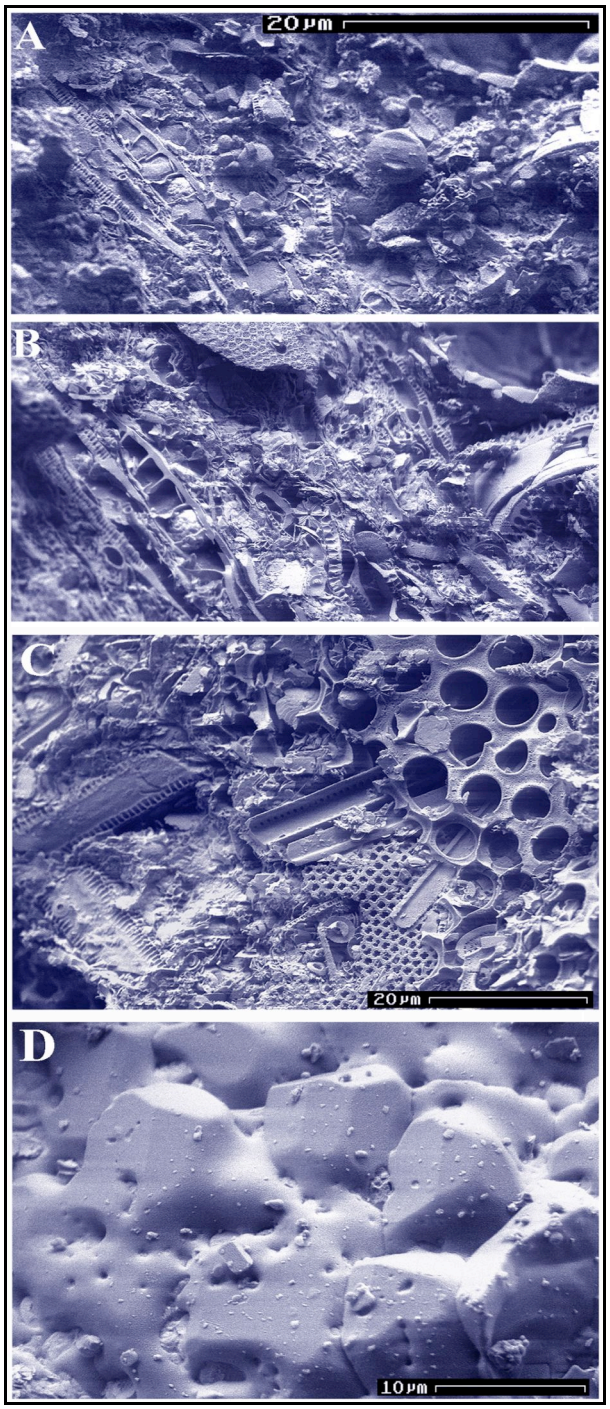

Figure 16. India NGHP-01 sample HYD 115. **A** and **B** show an 18 minute time lapse, where hydrate sublimation reveals the skeletal fragments below that make up the bulk of this sample. Hydrate grain boundaries in **A** are indistinguishable, but the hydrate fills the voids that are clearly exposed in **B**. A different section is shown in **C**. Finely crystalline hydrate also forms throughout this sample (**D**).

Despite the many thousands of CSEM images of natural gas hydrates archived to date, it's likely we've still just begun to scratch the surface in discovering the full range of textures, fabrics, and crystal habits displayed by natural gas-hydrate-bearing systems. So far, both the similarities and differences exhibited by gas hydrates from different localities have been quite startling. Each new batch of hydrate-bearing core typically arrives in an increasingly better state of preservation as recovery techniques continue to improve, so we are optimistic in further use of the CSEM technique to improve our understanding of gas hydrate formation in nature.

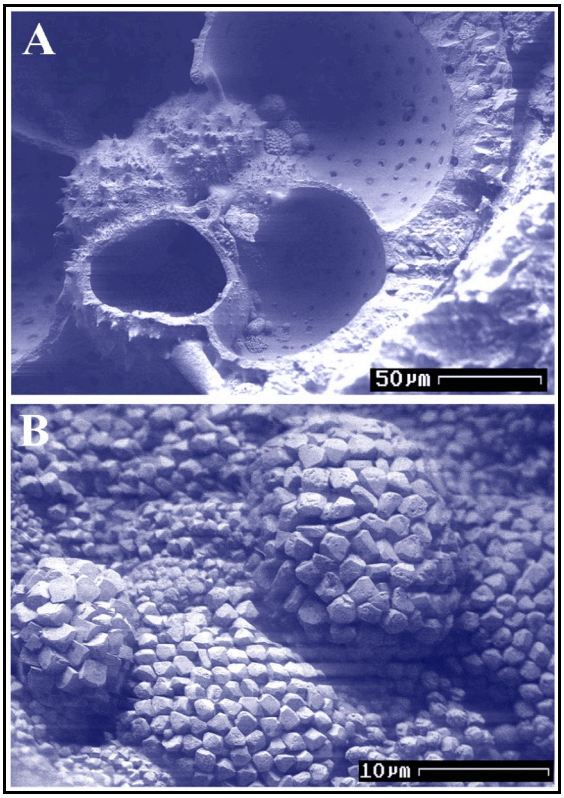

Figure 17. In several of the India NGHP-01 cores such as HYD 19 shown here, spheroidal accumulations of self-organized pyrite crystallites, called framboids, were often observed in the sediment portion or within chambers of skeletal fragments, as shown in **A**. Detailed view shown in **B**.

Acknowledgements. This work was supported in part by the DOE and by the USGS Gas Hydrate Project. We thank R. Oscarson and J. Pinkston of the USGS for technical assistance, and T. Lorenson and W. Waite (USGS) for helpful reviews of the manuscript. We also thank T. Kneafsey of Lawrence Berkeley Laboratory for providing CT x-ray scans of the NGHP-01 cores. Burt Chen (National Taiwan University) took image Fig. 10C.

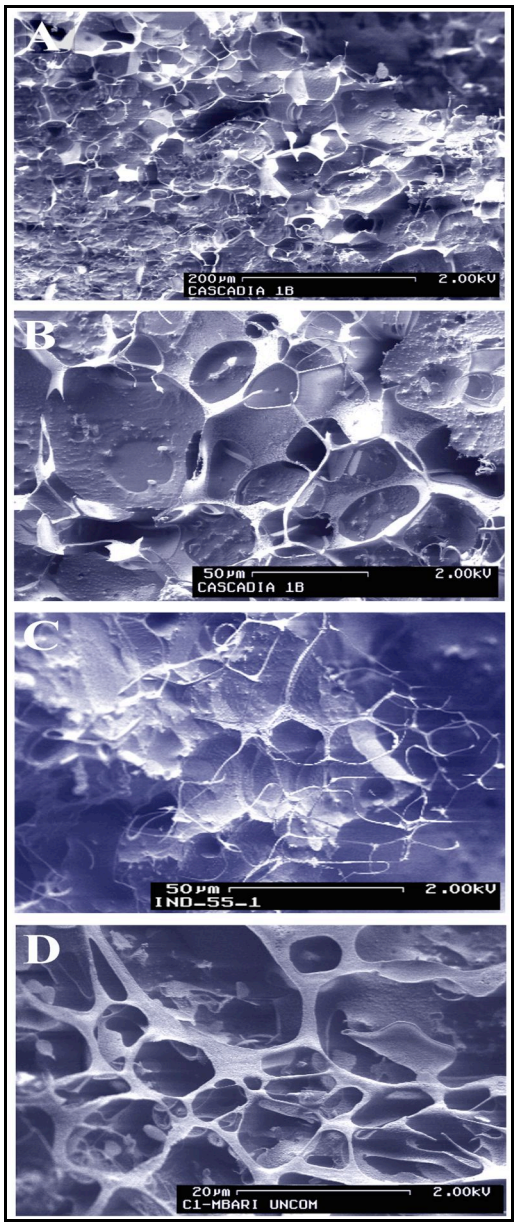

Figure 18. Dissociation features produced during recovery. Cascadia sample 1328B (**A**, **B**) and India NGHP sample 55 (**C**) both show frothy ice features near the sample surface. Virtually identical structures form in lab-made methane hydrate annealed at the seafloor (**D**) as well as in degassing volcanic melts upon quenching [17], suggesting these foam textures formed during rapid dissociation during recovery.

REFERENCES

[1] Kuhs W, Klapproth A, Gotthardt F, Techmer K, Heinrichs T. *The formation of meso- and macroporous gas hydrates*. Geophys. Res. Lett. 2000;27:2929-2932.

[2] Staykova D, Kuhs W, Salamatin A, Hansen T. *Formation of porous gas hydrate from ice powders: diffraction experiments and multi stage model*. Journal of Physical Chemistry B 2003;107:10299-10311.

[3] Klapproth A, Goreshnik E, Staykova D, Klein H, Kuhs W. *Structural studies of gas hydrates*. Canadian Journal of Physics 2003;81(1-2):503-518.

[4] Genov G, Kuhs W, Staykova D, Goreshnik E, Salamatin A. *Experimental studies of the formation of porous gas hydrates*. Am. Min. 2004;89:1228-1239.

[5] Kuhs W, Genov G, Goreshnik E, Zeller A, Techmer K, Borhmann G. *The impact of porous microstructures of gas hydrates on their macroscopic properties*. Proc. 14th Offshore and Polar Eng. Conference, Toulon, France, 2004; 31-35.

[6] Techmer K, Heinrichs T, Kuhs W. *Cryo-electron microscopic studies of structures and composition of Mallik gas-hydrate-bearing samples*. In: Scientific Results from the Mallik 2002 Gas Hydrate Production Research Well Program, Geological Survey of Canada, 2004; Bulletin. 585.

[7] Suess E, Borhmann G, Rickert D, Kuhs W, Torres M, Trehu A, Linke P. *Properties and fabric of near surface methane hydrates at hydrate ridge, Cascadia margin*. Proceedings of the 4th international Conference on Gas Hydrates, Yokohama, 2002;2:740-744.

[8] Stern L, Circone S, Kirby S, Durham W. *Application of Scanning Electron Microscopy to investigate growth and annealing of gas hydrates formed from melting ice.* Am. Min. 2004;89:1162-1175.

[9] Stern L, Circone S, Kirby S, Durham W. *Temperature, pressure, and compositional effects on anomalous or "self" preservation of gas hydrates*. Canadian Journal of Physics 2003; 81(1-2):271-283.

[10] Stern L, Circone S, Kirby S, Durham W. *SEM imaging of gas hydrate formation processes and growth textures, and comparison to natural hydrates of marine and permafrost origin.* In: Proc. 5th International Conf. on Gas Hydrates, Trondheim, 2005;1:300-309.

[11] Durham W, Kirby S, Stern L, Zhang W. *The strength and rheology of methane clathrate hydrate.* J. Geophysical Research 2003; 108(B4):2182- 2193.

[12] Durham W, Stern L, Kirby S, Circone S. *Rheological comparisons and structural imaging of sI and sII end-member gas hydrates and hydrate/sediment aggregates*. In: Proc. 5th Internat'l Conf. on Gas Hydrates,Trondheim, 2005;2:607-614.

[13] Circone S, Stern L, Kirby S, Durham W, Chakoumakos B, Rawn C, Rondinone A, Ishii Y. *CO_2 hydrate: synthesis, composition, dissociation behavior, and a comparison to sI CH_4 hydrate*. J. Phys. Chem. B 2003;107(23):5529-5539.

[14] Stern L, Kirby S. *Grain and pore structure imaging of gas hydrate from core MD02-2569 (W. Mississippi Site, Gulf of Mexico): a first look by SEM.* In, Winters W, Ed. Gas Hydrate and Paleoclimate Results from the RV Marion-Dufresne Cruise to the Gulf of Mexico July 2002. USGS Digital Data Series, Open-File Report 2004-1358.

[15] Stern L, Kirby S, Durham W. *SEM imaging of grain structure and phase distribution within hydrate-bearing intervals from JAPEX/JNOC/GSC et al. Mallik 5L-38.* In: Dallimore S and Collett T, Eds., Scientific Results from the Mallik 2002 Gas Hydrate Production Research Well Program, Geological Survey of Canada, 2004; Bulletin. 585, paper 31.

[16] Klapp S, Klein H, Kuhs, W. *First determination of gas hydrate crystallite size distributions using high-energy synchrotron radiation*. Geophy. Res. Letters 2007;34:L13608.

[17] Mangan M, Cashman K. *The structure of basaltic scoria and reticulite and inferences for vesiculation, foam formation, and fragmentation in lava fountains*. J. Volcanology and Geothermal Research 1996;73:1-18.

[18] Circone S, Kirby S, Stern L. *Direct measurement of methane hydrate composition along the hydrate equilibrium boundary*. J. Physical Chemistry B, 2005;109(19):9468-9475.